Proceedings of the 4th WSEAS International Conference on Fluid Mechanics and Aerodynamics, Elounda, Greece, August 21-23, 2006 (pp325-330)

Measurement of the Periodic Unsteady Flow in a Single-Blade Centrifugal Pump by PIV-Method

M. ZWINGENBERG, F.-K. BENRA (SUPERVISOR)
Department of Turbomachinery
University of Duisburg-Essen
D-47057 Duisburg
GERMANY

Abstract: - This paper reports results from the PIV-measurement of the flow field in a single blade centrifugal pump and the sequences how these results have been achieved. Eight different angle positions for three different blade heights at three different operating points have been investigated corresponding to former CFD-simulations of the flow field for this pump. Numerical results have been exemplary compared with the PIV-measurements. It is shown, that the agreement between CFD and PIV is quite good but there are also some areas of a higher deviation between PIV and CFD which are also shown in this paper.

Key-Words: - particle image velocimetry, single-blade impeller, periodic unsteady flow

1 Introduction

For the transport of sewage water, in most cases single-stage pumps with a single-blade geometry of the impeller are used. This is done due to the special composition of sewage water which partially contains large portions of fibers and solids. This fact requires a huge minimum free ball passage to avoid clogging and to guarantee an undisturbed operation of the pump. A great disadvantage of this impeller geometry is the generation of a strong hydrodynamic unbalance [1-4]. This unbalance is caused by generation of an asymmetric pressure distribution along the suction and the pressure side of the blade. After passing the blade and before leaving the casing, the flow interacts with the casing and generates a transient pressure field. This field produces a variable flow force which, in combination with the mechanical imbalances, causes vibrations, which may damage the pump or the attached piping. To avoid this, it is very important, to be able to simulate the flow in the pump in an appropriate way, so that different variations of impeller and casing can be computed and compared within a short time. In order to validate the CFD-results, PIV measurements for different operating points and different impeller positions were done at a test pump (parameters of the test pump in table 1) and the results were compared to the CFD-simulation.

Operating conditions	Value	Design parameters	Value
Q	146,16 m^3/h	D_{ann}	380 mm
H	8 m	D_{imp}	240 mm
n	1450 rpm	D_s	100 mm
n_q	51 rpm		

Table 1: Design parameters of the test pump

2 Nomenclature

Arabic letters

D	m	diameter
Q	l/s	volume flow rate
H	m	delivery head
SNR	-	signal to noise ration
n	min^{-1}	number of revolutions
x	-	cartesian coordinates
y	-	cartesian coordinates
z	-	cartesian coordinates
u	m/s	velocity in x-direction
v	m/s	velocity in y-direction
w	m/s	velocity in z-direction
t	s	time
f	s^{-1}	frequency

Greek letters

φ	deg	angle of rotation
ω	°/s	angular velocity
π	-	3.141592654
Δ	-	difference

Subscripts

des	design
ann	annular
imp	impeller
s	suction

3 PIV-Measurements

In order to validate the CFD-results, PIV-measurements were done at a test stand, which had been built under survey of Prof. Siekmann, Technical University of Berlin [5-7]. As it can be seen in figure 1, the stand contains the pump itself, the driving and the piping (length approx. 9m). Furthermore, a flowmeter and a

choke valve are integrated in the piping so that different operating points can be investigated. Between the pump and the outlet of the piping a flow straightener has been installed to reduce the turbulence in the holding tank.

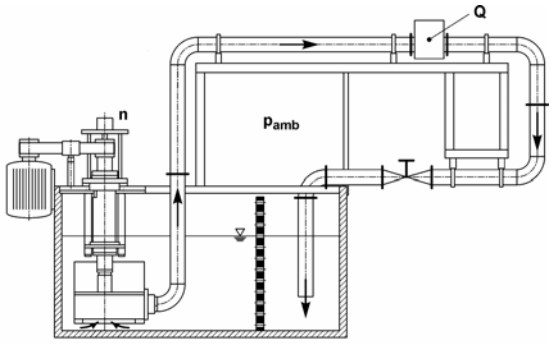

Figure 1: Test stand

In order to make PIV-measurements possible, the tank has to be equipped with windows at the side and at the bottom of the tank to guarantee optical access for the PIV-components. The impeller and the casing have been manufactured out of transparent plexi glass, so that there is no barrier for the laser light. The setup of the PIV-system can be seen in figure 2. The light source, which is not contained in this figure, was a 20Hz NewWave Solo Nd-Yag-Laser with a wavelength of 532nm and a maximum pulse energy per beam of about 120mJ. The light beam was extended by an optical lens to a laser light sheet of 2mm thickness. The CCD-camera which, was mounted below the pump, was equipped with a green filter, so that only those particles, which were illuminated by the laser light, could be detected. Thus, the influence of illumination through daylight could be significantly reduced.

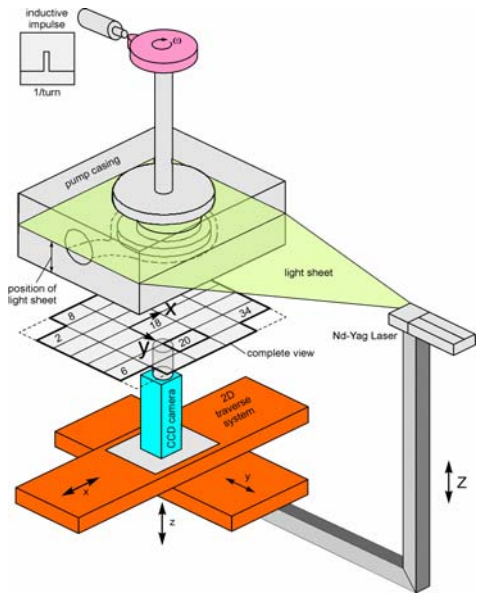

Figure 2: Setup of the PIV-system

The images taken by the CCD-camera had a size of 1024x1080 pixels with an 8 bit resolution of grey scale. For triggering the camera, a single inductive measured impulse is given per one rotation of the pump. Thus, only the 0°-position could be determined. In order to measure at different angle-positions, a time delay was used. According to the angular speed, the needed time-delay could be calculated, so that any angle could be adjusted according to the following formula.

$$\Delta t = \frac{\Delta \varphi}{2\pi f} \tag{1}$$

The camera was fixed on a 2-dimensional traverse system. This system was fixed on a table, which was able to lift the whole system including the laser light arm according to the required blade height. By moving the whole system in z-direction, the distance between light sheet and camera is constant, so that each image is of the same size. The area which is covered by one image is about 57mmx72mm which assures a high resolution of the flow. In order to cover the whole section, 35 single positions are needed, as it can be seen in figure 3. For each position, 20 pictures were taken to exclude random failure and strengthen the signal quality for further evaluations.

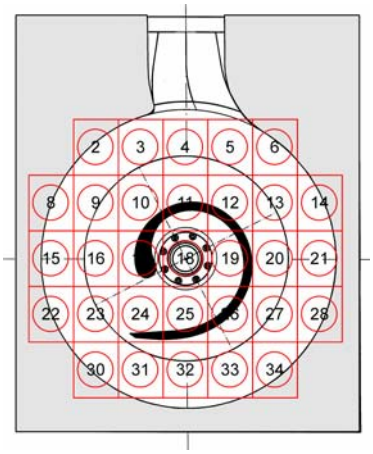

Figure 3: Partitioning of the measurement area

Though it was possible to integrate the traverse system into Dantec's PIV-measurement software FlowManager [10], the measurement of one section (35 images) could be automated. The PIV-measurements were done at three different operating points, Q/Q_{des}=50%; 100%; 125% for three blade heights, h/h_{blade}=25%; 50%; 75%; whereas the 25% position is near the hub and the 75% position is near the shroud. Altogether 700 PIV-images per section of one angle position were taken and 8 angle positions per operating point were investigated.

3 Evaluation Sequence

In order to achieve sufficient results out of a PIV-image, several evaluation steps must be done. These steps have to be chosen individually depending to a specific result which should be derived. The aim of this evaluation sequence is to be able to compare directly between the CFD-calculation and the PIV-measurements within one particular software, e.g. CFX or FlowMatch [9].

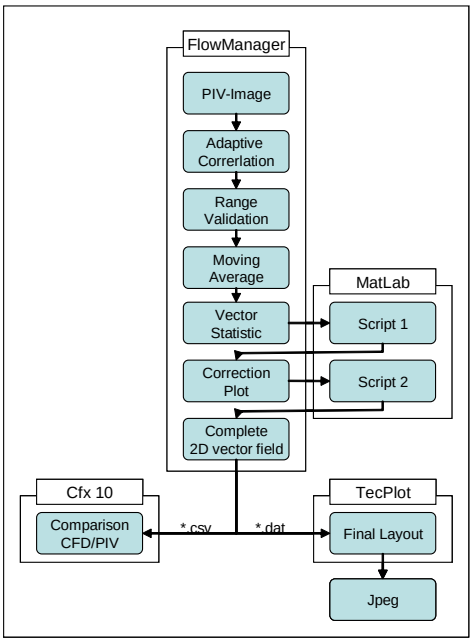

Figure 4: Evaluation Sequence

The first three steps were done for every single PIV-Image. These steps are an adaptive correlation, a range validation and a moving average procedure. The adaptive correlation has been chosen because it generates the better results compared to a cross correlation due to a shifting of the interrogation area, which significantly reduces the SNR for a high velocity gradient within a small area, e.g. at the trailing edge of the impeller. The final interrogation area of this correlation was 32x32 pixels with an overlapping of 50% in horizontal and vertical direction. For the offset of the interrogation area, the central difference method was chosen. Because of reflections at bubbles or bigger particles or cords due to shading in the image, the results of the adaptive correlation were still insufficient because of a big amount of outliers in the critical areas. In order to reduce this amount, a range validation was used. With this method, a range of velocities is defined, so that outliers which had an obviously too high velocity were sorted out. The boundaries for the velocities were chosen according to the CFD-simulation, but it turned out that a lower upper boundary of 13 $^{m}/_{s}$ was high enough to maintain the correct vectors and to sort out the outliers. By doing this, little gaps were generated in the flow field because of the exclusion of the outliers. The Moving Average method was used in order to fill these gaps and for smoothing the flow. This method detects too high velocity gradients in the flow field and can fill gaps by adding velocity vectors, which are calculated from the surrounding vectors. For this step, an averaging area of 3x3 pixels and an acceptance factor of 0.1 were chosen. Three iteration steps were carried out to achieve a sufficient result. Figure 5 shows the original PIV-image and in figure 6 the result of these first three steps can be seen. The red vectors are outliers and the green ones are substituted vectors resulting from the moving average method.

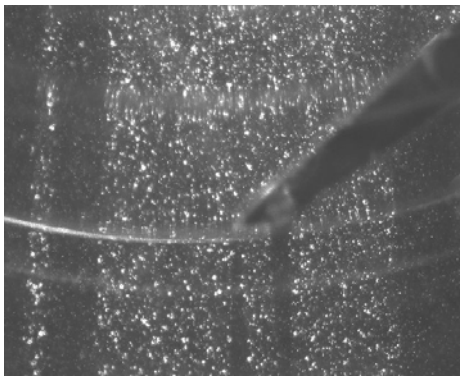

Figure 5: PIV-Image

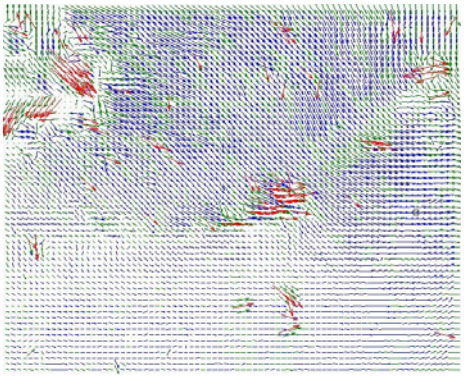

Figure 6: Moving Average Plot

In order to minimize random failures, which are included in most images [8], a vector statistic was computed for every single setup. By this step, the information about the u- and v-components of every gridknot-position were arithmetical averaged for the 20 images of each setup. In this way, the quality of the vector plot rose strongly. To highlight the trailing edge or other parts of the blade or the casing and to remove those obviously false vectors at the area of the blade, a mask was generated. This mask was manually drawn and laid over the vector statistics. The masking was effective if 50% or more of the interrogation area was covered. In this case, the FlowManager [10] internal status information for these vectors is changed. By exporting the masked vector statistics to MatLab [11], all vectors with a specified status information were set to zero. This step is not possible in Flow Manager, but the resulting plot from the

MatLab-Script is exported back to FlowManager, so that the Correction Plot is available for further calculations in FlowManager. The result of this step can be seen in figure 7.

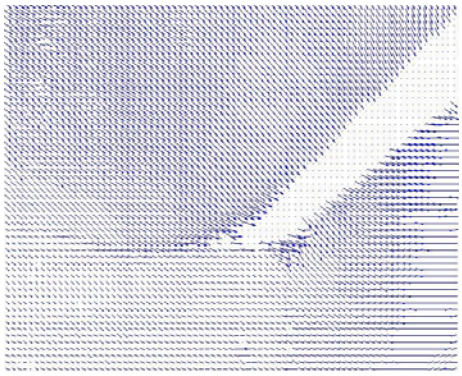

Figure 7: Correction Plot

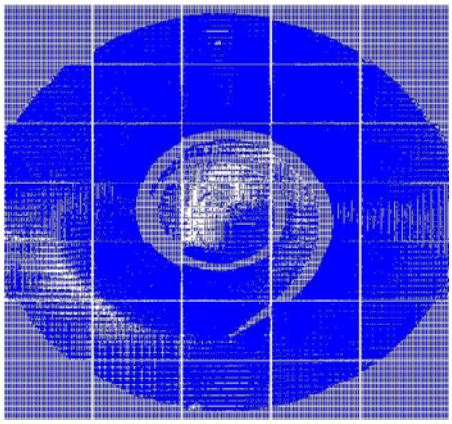

Figure 8: Mid-Span Plot

Now all 35 correction plots of one setup were exported to MatLab. The MatLab script generated four matrices for the x-, y-, u- and v-components within one matrix. Through this method, an x-y-grid for the whole mid-span section was generated within about 150000 vectors. This axis normal plane (fig. 8) was saved for further purposes as a MatLab file and then exported back to FlowManager. At this point, the evaluation in FlowManager is concluded. For obtaining a picture of this axis normal plane and to visualize in this picture for instance streamlines, lines of constant velocities, or other interesting facts, the data can be exported to TecPlot [12]. At the end of this step one can obtain a picture, which allows the qualitative comparison between simulation and measurement. To calculate the deviation between numerical and experimental results, the data has to be exported to CFX or FlowMatch. Therefore the FlowManager data has to be exported as a comma separated value file with a special header. This file includes some extra information such as the z-component of the plane or the fact that all w-velocity vectors are set to zero. With this setup of software it is now possible, to compare the data of PIV and CFD in a quantitative way and to come to a definitive conclusion about the differences between measurement and simulation.

4 Comparison of CFD- and PIV-Data

The PIV-Measurements were done to validate the results of the CFD-simulation. And at first view, the congruence between PIV and CFD seems to be quite good. But of course, there are some differences which one has to keep in mind for further evaluations of the CFD-results. The first difference which attracts attention is that the level of velocity in the whole mid-span-section of the PIV-data seems to be about 1.5-2 $^{m}/_{s}$ below the velocities of the simulation. This phenomenon can be observed, for example, at the φ=90° position (fig. 9a) in the outer areas of the casing, where the velocities are quite low. In the PIV-Image the area of the lowest velocities is a lot bigger than calculated. As for the CFD-result, the velocity near the casing walls is as low as the velocity of the PIV-data for this area. But with regard to an increasing distance to the casing walls, the velocity for the CFD-data began to rise about 1.5 $^{m}/_{s}$ in relation to the PIV-data.

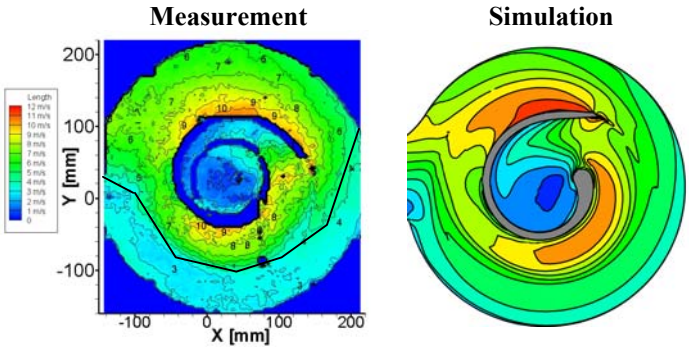

Figure 9a: PIV and CFD velocity field at mid span (Q/Q_{des}=100%, n=1450 rpm, φ=90°)

The two-dimensional expansion of this area is quite similar to the expansion of the area of lowest velocity for PIV-data. Thus, in this case the CFD-simulation gives a very good overview of the flow, despite the higher velocities. Another example of areas of same extension can be given by the areas of the highest velocities on the pressure side of the blade. They are nearly at the same position as for CFD and PIV, but again the value of the velocity is lower for the PIV-data. An interesting and contrary aspect to this is the area between the trailing and the leading edge of the impeller. For the φ=213° (fig. 9b) and the φ=258° (fig 9c) position there is an area of constant velocity for the PIV and the CFD data. But contrary to the former observations, the velocities in this area are higher for the PIV-data. The difference between PIV and CFD for this area is about 1 $^{m}/_{s}$. Despite this, the area of lower

velocities in figure 9c shows a very good agreement between CFD and PIV. The extension is very similar and the flow from the trailing edge to the casing seems to be congruent for PIV and CFD.

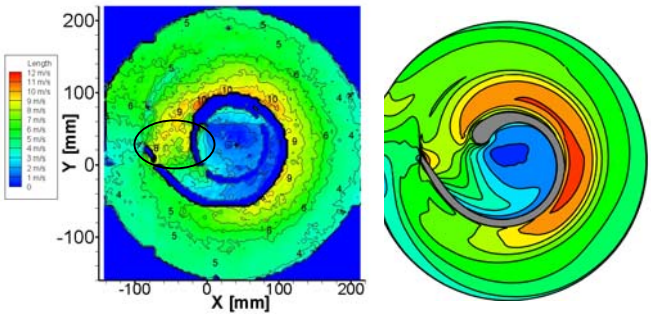

Figure 9b: PIV and CFD velocity field at mid span (Q/Q_{des}=100%, n=1450 rpm, φ=213°)

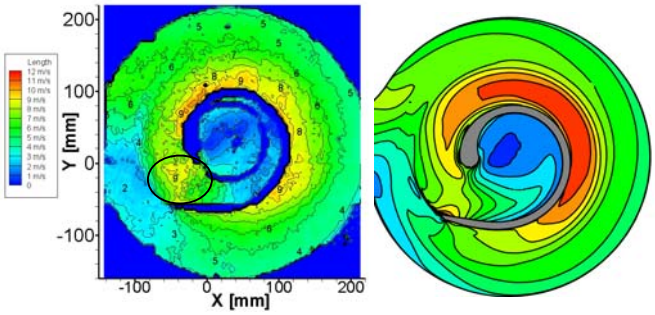

Figure 9c: PIV and CFD velocity field at mid span (Q/Q_{des}=100%, n=1450 rpm, φ=258°)

If one looks at the PIV-image (fig. 9b), there seems to be one area which extends from the trailing edge to the leading edge and goes on to the pressure side of the blade with nearly a constant velocity. For the CFD-simulation, there is an area between leading and trailing edge with relatively low velocities (approx. 6 $^{m}/_{s}$) and an area with higher velocities (9-10 $^{m}/_{s}$) on the pressure side of the blade. By analyzing the φ=348° position (fig. 9d), one can see again a general congruence between CFD and PIV. All remarkable areas, such as areas of very low or very high velocities, seem to be of the same extension and at the same position. This can be seen for example in the upper marked area in figure 9d. The gap between the areas of high velocities can be seen clearly, too. But of course, the velocities of the PIV-data are a little lower than they are with regard to the CFD-data. Again the critical area is the area between leading and trailing edge of the impeller. For the CFD-data, in this area there is a stable field of a constant velocity (approx. 6 $^{m}/_{s}$), while for the PIV-data this field has higher velocities and it seems to be very unstable. Thus, there are some fragmented areas of the same velocity, but there is no consistent area as it can be seen in the CFD-data. Another interesting fact is that for this position and contrary to the φ=90° position (fig. 9a), the area of the lowest velocity has nearly the same extension for CFD and PIV, while for the φ=90° position this area was a lot larger in the PIV-data. By contemplating all four images at once, it is noticeable that the velocities in the outer areas of the casing of the CFD-data are close to the velocities of the PIV-data. But with a smaller radius and an approaching to the impeller, the difference between CFD and PIV rises. The maximum difference between the two data-sets is at the pressure side of the impeller. This maximum difference seems to rise with a progressive angle of rotation.

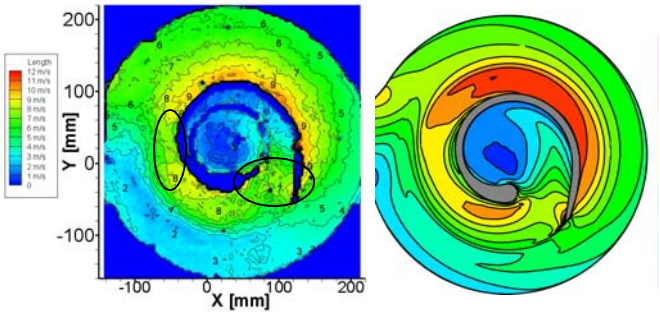

Figure 9d: PIV and CFD velocity field at mid span (Q/Q_{des}=100%, n=1450 rpm, φ=348°)

For different blade heights, the congruence between CFD and PIV is not as good as for mid span. Near the hub (fig. 10a), the area of high velocities (CFD) at the pressure side of the blade is neglectably small in the PIV-data. In the PIV-image, there is only a small area with lightly higher velocities, but its extension is very small in relation to the CFD-simulation. But again, the center of each area is nearly the same for PIV and CFD. This applies likewise to the area of higher velocities at the trailing edge of the impeller. For this area, velocity, extension and center of the area are nearly identical for both datasets. But for the rest of the flow field the congruence is suboptimal. For the PIV-data, there is a very homogeneous velocity field while the field of the CFD-data has salient minima and maxima, for example the area of high velocities at the pressure side connection.

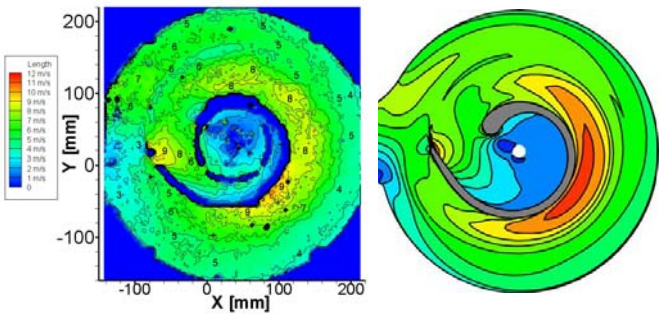

Figure 10a: PIV and CFD velocity field near hub (Q/Q_{des}=100%, n=1450 rpm, φ=213°)

The congruence between CFD and PIV near the shroud (fig. 10b) is better than near the hub but not as good as

for the mid span. The areas of highest velocities at the leading edge of the impeller are very similar in terms of extension and position. But the area of slightly lower velocities behind this area is a lot larger for the CFD-data than for the PIV-data. The rest of the flow field seems to be very congruent and confirmed the CFD-data, beside the marked area. As it was shown, this is the critical part for the comparison between CFD and PIV. As for the PIV-image, there is a pronounced area of lowest velocities at the suction side of the impeller which can not be seen in the CFD-data. For this area, the general velocity difference between CFD and PIV is about 2-3 $^{m}/_{s}$.

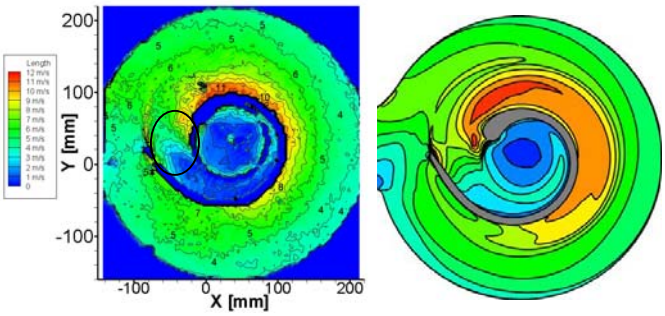

Figure 10b: PIV and CFD velocity field near shroud (Q/Q_{des}=100%, n=1450 rpm, φ=213°)

With regard to the analysis of the sections at middle height, near the hub and near the shroud, the 3-dimensional character, especially in z-direction, of the flow seems to be pronounced in a stronger way than the CFD-analysis has shown. With regard to the complete comparison between CFD and PIV, there are only a few areas with a greater difference between the two data sets. Despite this, a very good agreement between simulation and measurement has been obtained, for the rest of the flow field.

5 Conclusion

PIV-measurements of the flow in a single-blade centrifugal pump were done and the results were compared to the results of the numerical simulation in an qualitative way. For all positions, a generally very good agreement between CFD and PIV could be shown. Of course, the velocities measured by PIV are a little lower than estimated. This leads to the several assumptions that maybe the losses on the surfaces of the casing and the impeller are higher or that the gap between shroud and casing is bigger than estimated and by this way additional losses are generated. Another possibility is that the energy transfer of the impeller is not as good as estimated. By comparing the datasets, some critical areas could be detected, such as the area between leading and trailing edge or the suction side of the blade. For these areas, the flow field for CFD and PIV shows a bigger deviance, so that these areas should be analyzed in a more detailed way in the future. Furthermore, the analysis of the PIV-data should be done in a quantitative way by importing the datasets to CFX or FlowMatch, to get concrete values for the deviance between CFD and PIV.

References:

[1] Agostinelli, A.; Nobles, D.; Mockridge, C.R.: An Experimental Investigations of Radial Thrust in Centrifugal Pumps, Transactions of the ASME, Journal of Engineering for Power, Vol. 82, No. 2, 1960

[2] Okamura, T.: Radial Thrust in Centrifugal Pumps with Single-Vane-Impeller, Bull. of JSME 23, No. 180, 1980

[3] Aoki, M.: Instantaneous Interblade Pressure Distributions and Fluctuating Radial Thrust in a Single-Blade Centrifugal Pump, Bulletin of the JSME 27, No. 233, 1984

[4] Gülich, J.; Jud, W.; Hughes, S.F.: Review of Parameters Influencing Hydraulic Forces on Centrifugal Impellers, Proc. Inst. Mech. Engineers, Vol. 201, No. A3, 1987

[5] Ulbrich, C.: Experimentelle Untersuchung der Pumpencharakteristiken und Geschwindigkeitsfelder einer Einschaufelrad-Kreiselpumpe, Dissertation TU Berlin, 1997

[6] Scheffler, T.; Siekmann, H.: Multi Field DPIV Measurements in a Single Blade Pump, 7th International Conference on Laser Anemometry Advances and Applications, Karlsruhe 1997

[7] Siekmann, H.; Scheffler, T.: Unsteady Flow Field Investigations by Means of Digital Particle Image Velocimetry, The Fifth Asian International Conference On Fluid Machinery, Seoul, Korea, 1997

[8] Jonas Bolinder, Optimization of PIV in flows with strong velocity gradients, http://www.piv.de/papers/bolinderlundpivopt.pdf

[9] http://www.dantecdynamics.com/FlowMatch/

[10] http://www.dantecdynamics.com/piv/system/software/Index.html

[11] http://www.mathworks.com/products/matlab/description1.html

[12] http://www.tecplot.com/products/tecplot/tecplot_main.htm